ScienceDirect

IFAC Papers Online

CONFERENCE PAPER ARCHIVE

IFAC PapersOnLine 51-24 (2018) 480–487

Fault detection and isolation of pitch actuator faults in a floating wind turbine

Christian Tutivén * **Yolanda Vidal** * **Leonardo Acho** * **José Rodellar** *

* *Control Dynamics and Applications, Departament de Matemàtiques, Escola d'Enginyeria de Barcelona Est, Universitat Politècnica de Catalunya, 08930, Spain (e-mail: {christian.tutiven, yolanda.vidal, leonardo.acho, jose.rodellar}@upc.edu).*

Abstract: In this work, the problem of detection and isolation of pitch actuator faults in wind turbines (WTs) is addressed. First, interval observers are used by means of the Luenberger observer to obtain an upper and a lower estimated bounds. The main advantage of this approach is that the new bounds enclose the real output measurement within a bounded interval in a guaranteed way under consideration of the uncertainties (in this case noise in the pitch measurement). Finally, residual signals are obtained and processed to detect and isolate the different faults. The efficiency of the proposed approach is demonstrated through simulation with the 5MW floating offshore (barge) WT benchmark model given by the aero-lastic wind turbine simulator–FAST. This software is designed by the U.S. National Renewable Energy Laboratory and is widely used in research and industry.

Keywords: Fault detection; Fault isolation; Interval observer; Residual signal.

1. INTRODUCTION

Wind power is having a rapid growth and is one of the renewable energy sources that has received enormous attention to alleviate the global demand for fossil fuels and the resulting concerns about environmental issues [Gsanger and Pitteloud (2012)]. Moreover, it is likely that offshore wind power will increase more than onshore as vast expanses of open sea are available, minmizing visual and noise annoyances and with higher and steadier winds [Jonkman (2007)]. However, offshore WTs are expensive and far from the living zones. Hence, both the size and location factors come into play and lead to increased maintenance challenges. The cost of operation and maintenance of offshore WTs is among 15-35 % of the total cost; from this, 80% are due to unplanned maintenance [Leithead and Dominguez (2005)]. Thus, research into methods of fault detection and isolation (FDI) and fault tolerant control (FTC) are the crux of the matter to maximize productivity of WTs [Odgaard and Johnson (2013); Chaaban et al. (2014)].

A monitoring system which is used to detect faults and also to determine the type, size and location of the most possible faults, as well as its time of detection, is called a fault diagnosis system. Fault diagnosis is very often considered as FDI, in the literature. Such a FDI system normally consists of the following tasks [Chen and Patton (2012)]:

- **Fault detection:** to make a binary decision - the system is healthy or a fault appeared.
- **Fault isolation:** to determine the location of the fault, e.g., which sensor or actuator has become faulty.
- **Fault identification:** to estimate the size and type or nature of the fault.

The aim of FDI is to detect faults as early as possible, while at the same time false alarms –for example due to measurement noise –must be avoided to minimize unnecessary WTs shutdowns. Thus, robustness and simultaneously high fault sensitivity are the most important goals. A first benchmark challenge about fault detection and isolation of wind turbines was presented in [Odgaard et al. (2013)]. In this work, Odgaard and Stoustrup provide a benchmark for researchers working in the field of fault diagnosis and fault-tolerant control. Their work presented different types of faults and test sets. These faults cover sensors, actuators, and process faults in different parts of the WT. After the announcement of the results of the first benchmark, a second challenge was presented in [Odgaard and Johnson (2013)]. In this challenge, the WT is modeled in FAST [Jonkman et al. (2005)]. This means that a higher-fidelity, more detailed, aerodynamic, structural and realistic WT model was used and thus the results were of greater relevance for the wind industry. Also, the fault scenarios were updated and additional information detailing their relevance was provided. One type of the presented faults is the pitch system failure which is the predominant error being responsible for more than 20% of the failures per turbine per year [Tavner (2012)]. In

⋆ This work has been partially funded by the Spanish Ministry of Economy and Competitiveness through the research projects DPI2014-58427-C2-1-R, DPI2015-64170-R(MINECO/FEDER), and by the Catalonia Government through the research project 2014 SGR 859.

⋆⋆This work was done in a research stay in the Institute of Control Systems (Head: Prof. Dr.-Ing. Soren Hohmann) of the Karlsruhe Institute of Technology (Karlsruhe, Germany), where we worked with interval observers models for FDI in WTs.

Peer review under responsibility of International Federation of Automatic Control.
10.1016/j.ifacol.2018.09.620

this work, three common pitch actuator faults proposed in [Odgaard and Johnson (2013)] are used to test the proposed FDI system.

The FDI methods can be classified as into three categories: signal processing based, data based (techniques based on knowledge) and model based [Puig et al. (2004)]. In the latter case, which is the approach used in this thesis, FDI makes use of mathematical models of the system to represent the relations between measured input signals and output signals to extract information on possible changes caused by faults. These relations mostly in form of process model equations but can also be causalities in form of, e.g. if-then rules. Model-based FDI approach is the subject of intensive research activities for WTs. For example, observer-based schemes are provided in [Chen et al. (2011)]. Analytical redundancy relations (ARRs) and interval observers are used in [Sanchez et al. (2015)] and in [Odgaard et al. (2015)] to detect faults in WTs. In [Blesa et al. (2014)] fault detection is based on interval observers and unknown, but bounded, description of the noise and modeling errors. An automated fault detection and isolation scheme design method is presented in [Svärd and Nyberg (2011)]. The work in [Pisu and Ayalew (2011)] is based on parity equations. Data-driven methods are used in [Dong and Verhaegen (2011)]. Finally, [Kiasi et al. (2011)] is based on a generalized likelihood ratio method.

Using appropriate system models, for example, interval models, and state-set observation techniques, uncertainties in both measurements and system models can be considered. This work uses the approach of interval observers which appeared in the last two decades as an alternative methodology for robust state estimation. It is an interesting class of observers that can be used to estimate upper- and lower-bounds on the state value of a given system at any given time [Gouzé et al. (2000), Rapaport and Gouzé (2003)]. The reason for using such observers lies in the fact that when the observed system is subject to disturbances or uncertainties, estimation errors are often unavoidable, unless decoupling is possible. When this happens, it becomes unclear in which region the state currently lies [Briat and Khammash (2016)]. Interval observers resolve this problem by estimating an upper and lower bound on the current state-value and defining an interval where the state lies at any given time.

In model-based FDI, it is typical that a fault is detected based on an analytical residual signal. Residuals are created to show a characteristic response to certain system faults. Thus, they allow not only fault detection, but also the separation of different faults, commonly known as fault isolation. The residual must be a signal that is close to zero in the absence of a fault, and significantly affected in the presence of faults [Vidal et al. (2012), Liberatore et al. (2006), Besançon (2003)]. The main components of a fault detection system are the following [Vidal et al. (2012), Liberatore et al. (2006)]: a residual generator signal, residual evaluation method, and a prescribed threshold to decide whether a fault occurs or not [Vidal et al. (2012), Liberatore et al. (2006), Edwards et al. (2000)]. Also, model-based FDI can be classified in two different approaches. The active approach aims at generating residuals that are sensitive to faults, while effects of disturbances not representing faulty system behavior are suppressed as far as possible [Wolff et al. (2008)]. On the other hand, the passive approach aims at generating residuals such that the effects of measurement and model uncertainties can be accounted for in the subsequent residual evaluation stage of the diagnosis algorithm [Wolff et al. (2008)]. A good overview of robustness issues in active and passive approaches can be found in [Puig et al. (2000)].

The purpose of this work is to detect and isolate different pitch actuator faults by bring interval observers [Krebs et al. (2016b)] to generate a residual signal that is robust against uncertainties (e.g. blade position measurement noise).

The document is organized as follows. In Section 2 the used wind turbine benchmark model is introduced. In Section 3 the proposed fault detection and isolation method based on interval observers is presented. The simulation results obtained with the proposed approach applied to the advanced WT benchmark are summarized in Section 4 and concluding remarks are given in Section 5.

2. REFERENCE WIND TURBINE

Several FAST models of real and composite wind turbines of varying sizes are available in the public domain. In this work, the barge-offshore version of a large WT, described by [Jonkman et al. (2009)], that is representative for real utility-scale sea-based multi-megawatt turbines is used. This WT is a conventional three-bladed, upwind, variable-speed, variable pitch-controlled turbine. The main properties of this turbine are listed in Table 1.

Table 1. **WT Characteristics.**

Rated power (P_n)	5 MW
Rotor type, blades	Upwind / 3 blades
Hub height	90.0 m
Rotor, hub diameter	126 m/3 m
Cut in, Rated, Cut-Out Wind Speed	3 m/s, 11.4 m/s, 25 m/s
Gearbox ratio	98
Nominal generator speed ($\omega_{g,n}$)	1173.7 rpm
Barge platform length	40 m
Barge platform width	40m
Barge platform height	10 m
Barge platform draft	4 m
Barge platform mass	5,452,330 kg
Water depth	150 m

The full non-linear model of the NREL 5MW WT [Jonkman et al. (2009)] mounted on a barge platform NREL model [Jonkman (2007)] is simulated using FAST, while the controllers are implemented in Matlab/Simulink. In the simulations, new wind datasets are generated in order to capture a more realistic turbulent wind simulation and, thus, to test the turbine controllers in a more realistic scenario. The turbulent-wind simulator TurbSim [Jonkman (2009)], developed by NREL, is used. Simulations were conducted for a realistic wind speed sequence with a mean speed of 18 m/s, turbulence intensity of 15%, run time of over 1300 s, and finally the reference height (where the mean wind speed is simulated) is set to 90.25 m. This wind speed sequence and the waves elevation are illustrated in Figure 1. The rated and cutout wind speeds are 11.4 m/s and 25 m/s, respectively. Thus, the wind profile lies in the above rated region. The water depth

at the assumed installation site is 150m, the height of the wave is 3.67 m, and the peak spectral period of the incident waves is set to 13.37 s. These values correspond to the same location analyzed by [Jonkman (2007)] in the North Sea near Scotland. All simulations use the same wind and wave profiles.

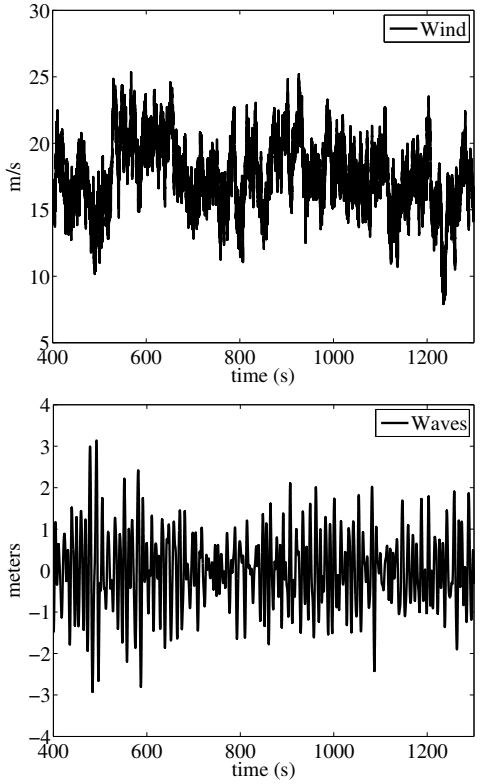

Fig. 1. Wind speed (m/s) and waves elevation (m).

2.1 Generator-converter actuator model

The generator and converter dynamics can be modeled by a first-order differential system [Odgaard et al. (2013)]:

$$\dot{\tau_g}(t) + \alpha_{gc}\tau_g(t) = \alpha_{gc}\tau_c(t), \tag{1}$$

where τ_g is the generator torque, τ_c is the torque reference to the generator (given by the controller), and α_{gc} is the generator and converter model parameter (in the simulations $\alpha_{gc} = 50$ [Jonkman et al. (2009)]). The signal given by the controller is saturated and rate limited and called $\hat{\tau}_c$, see Figure 4. The electrical power produced by the generator can be modeled by

$$P_e(t) = \eta_g\omega_g(t)\tau_g(t), \tag{2}$$

where $\eta_g = 0.98$ is the generator efficiency and ω_g is the generator speed measurement.

2.2 Pitch actuator model

The hydraulic pitch system can be modeled by a second order system [Odgaard and Johnson (2013)], with reference angle $\hat{\beta}_c$ and actual pitch angle β_i (output) as

$$\ddot{\beta}_i(t) + 2\zeta\omega_n\dot{\beta}_i(t) + \omega_n^2\beta_i(t) = \omega_n^2\hat{\beta}_c(t), \tag{3}$$

where ζ is the damping factor and ω_n is the natural frequency. This model is used for each pitch actuator ($i = 1, 2, 3$).

The system can be rewritten in state-space representation as

$$\dot{x}(t) = A \cdot x(t) + B \cdot \hat{\beta}_c(t), \tag{4}$$
$$\beta_i(t) = C \cdot x(t), \tag{5}$$

leading to,

$$A = \begin{pmatrix} 0 & 1 \\ -\omega_n^2 & -2\zeta\omega_n \end{pmatrix} \tag{6}$$
$$B = \begin{pmatrix} 0 \\ \omega_n^2 \end{pmatrix} \tag{7}$$
$$C = (1\ 0) \tag{8}$$

For the healthy case, the parameters $\zeta = 0.6$ and $\omega_n = 11.11$rad/s are used [Odgaard and Johnson (2013)].

2.3 Fault Description

Faults in a WT have different degrees of severity and accommodation requirements. A safe and fast shutdown of the WT is necessary for some of them, while for others, the system can be reconfigured to continue electrical power generation. Variable structure controllers can be applied in the case of failures that gradually change the system's dynamics. In this work, pitch actuator faults are studied as they are the actuators with the highest failure rate in WTs [Chaaban et al. (2014)]. A fault may change the dynamics of the pitch system by varying the damping factor and the natural frequencies from their nominal values to their faulty values in (3). The parameters for the pitch system under different conditions are given in Table 2. The normal air content in the hydraulic oil is 7%, whereas the high air content in the oil fault case (F1) corresponds to 15%. Pump wear (F2) represents the situation of 75% pressure in the pitch system, while the parameters stated for hydraulic leakage (F3) correspond to a pressure of only 50%.

Table 2. Parameters for the hydraulic pitch system under different conditions [Chaaban et al. (2014)].

Faults	ω_n (rad/s)	ζ
Fault-Free (FF)	11.11	0.60
High air content in oil (F1)	5.73	0.45
Pump wear (F2)	7.27	0.75
Hydraulic leakage (F3)	3.42	0.90

2.4 Baseline Control Strategy

The 5 MW reference WT given by FAST contains torque and pitch controllers for the full load region. In this work, the usual baseline control strategy described in [Jonkman et al. (2009)] is replaced by its modification described in [Jonkman (2010)], with the objective of eliminating the potential for negative damping of the platform-pitch mode and improving the floating turbine systems response (e.g. generated power). In this section, we recall these

controllers and refer to them as the baseline torque and pitch controllers.

The first modification is a change in the generator-torque control strategy when operating at rated power (i.e. full load region, also called region 3). That is, the new control law in region 3 is set to a constant generator-torque signal (rated toque),

$$\tau_c(t) = 43093.55\text{Nm}. \tag{9}$$

With this change, the generator-torque controller does not introduce negative damping in the rotor-speed response (which must be compensated by the blade-pitch controller), and so, reduces the rotor-speed excursions that are exaggerated by the reduction in gains in the blade-pitch controller. This improvement, though, comes at the expense of some overloading of the generator, as power increases with rotor-speed excursions above rated. Larson and Hanson [Larsen and Hanson (2007)] have demonstrated the effectiveness of this modification.

To assist the torque control with regulating the wind turbine electrical power output while avoiding significant loads and maintaining the rotor speed within acceptable limits, a collective pitch controller is added to the generator speed tracking error. The pitch controller uses the generator speed measurement as input. To mitigate high-frequency excitation of the control system, we filtered the generator speed measurement, using a recursive, single-pole low-pass filter with exponential smoothing as proposed by [Jonkman et al. (2009)]. The collective blade pitch gain scheduling PI-controller (GSPI) is one of the first well-documented controllers and it is used in the literature as a baseline controller to compare the obtained results. This GSPI control is a collective pitch controller that compensates the nonlinearities in the turbine by changing the controller gains according to a scheduling parameter. This controller was originally developed for the standard land-based 5MW turbine, see [Jonkman et al. (2009)]. The GSPI control has the generator speed as input and the pitch servo set-point, β_c, as output. That is,

$$\beta_c(t)=K_p(\gamma)(\hat{\omega}_g(t) - \omega_{g,r}(t))+K_i(\gamma)\int_0^t(\hat{\omega}_g(t) - \omega_{g,r}(t))d\tau, \quad i = 1, 2, 3, \tag{10}$$

where $\omega_{g,r}$ is the reference generator speed (usually the nominal value is used) and the scheduling parameter γ is obtained by averaging the measurements of all pitch angles as

$$\gamma = \frac{\sum_{i=1}^{3} \beta_i(t)}{3}. \tag{11}$$

The second modification is a reduction of gains in the blade-pitch-to-feather control system. In [Larsen and Hanson (2007)] is shown that the smallest controller-response natural frequency must be lower than the smallest critical support-structure natural frequency to ensure that the support-structure motions of an onshore floating wind turbine (OFWT) with active pitch-to-feather control remain positively damped. The new reduced proportional gain at minimum blade-pitch setting is 0.006275604 and the reduced integral gain at minimum blade-pitch setting is 0.0008965149 [Jonkman (2010)]. The gain-correction factor in the gain-scheduling law of the blade-pitch controller is unaffected by this change. Finally, to not exceed the mechanical limitations of the pitch actuator, the input signal β_c is saturated to a maximum of $\hat{\beta}_c = 90°$ and a rate limit of $\Delta\hat{\beta}_c = 8°/\text{s}$ [Jonkman et al. (2009)]. It is important that the control design takes into account these actuator limits. Otherwise, undesirable effects, such as transient response, degradation of the closed-loop performance, and even closed-loop instability, can appear [Kapila and Grigoriadis (2002)].

3. FAULT DETECTION AND ISOLATION

3.1 Interval Observer

Consider the system (4),(5) and the actual blade position measurement disturbed by an unknown noise $n(t)$,

$$\beta_{i,n}(t) = C \cdot x(t) + n(t). \tag{12}$$

To design the interval observer models, consider the pitch actuator Luenberger observer (as given in Figure 2), leading to,

$$\begin{gathered}\dot{\hat{x}}(t) = (A - LC) \cdot \hat{x}(t) + B \cdot \hat{\beta}_c(t) + L \cdot \beta_{i,n}(t), \\ \hat{x}(0) = \hat{x}_0,\end{gathered} \tag{13}$$

where $\hat{\beta}_c(t)$ is the known pitch actuator input signal, and L is the observer gain.

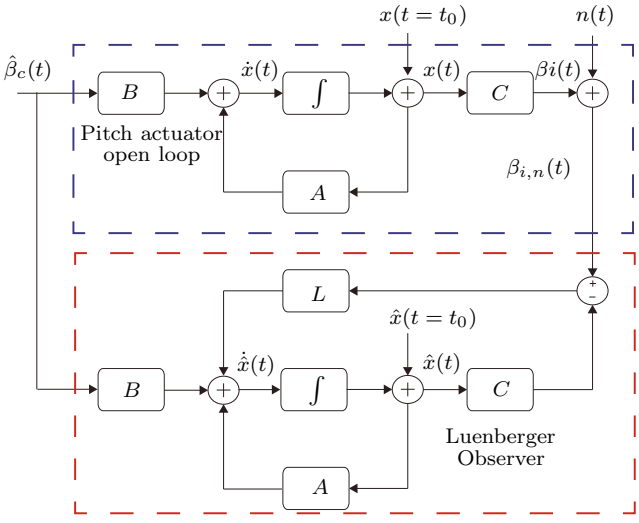

Fig. 2. Luenberger observer block diagram.

The aim is to find a lower bound $\underline{\beta_{i,n}}(t)$ and upper bound $\overline{\beta_{i,n}}(t)$ for the output measurement, considering the unknown white random noise such that

$$\underline{\beta_{i,n}}(t) \leq \beta_{i,n}(t) \leq \overline{\beta_{i,n}}(t), \tag{14}$$

$$max\{\beta_{i,n}(t) - \underline{\beta_{i,n}}(t), \overline{\beta_{i,n}}(t) - \beta_{i,n}(t)\}. \tag{15}$$

At this, $\underline{\beta_{i,n}}(t)$ denotes the output of the interval observer for the lower bound and $\overline{\beta_{i,n}}(t)$ denotes the output of the interval observer for the upper bound. The input

signal (given by the controller) is assumed to be exactly known. Since $[\beta_{i,n}]$ is an interval, we can take unknown-but-bounded measurement noise (η) into account [Wolff et al. (2008); Krebs et al. (2016b)]:

$$|n(t)| \leq \eta, \quad \eta \in \mathbb{R}, \tag{16}$$

$$[\beta_{i,n}] = [\beta_{i,n}(t) - \eta, \beta_{i,n}(t) + \eta] = [\underline{[\beta_{i,n}]}(t), \overline{[\beta_{i,n}]}(t)]. \tag{17}$$

Therefore, the only assumption on the measurement uncertainty is that it is bounded. No additional assumptions, for example, about the stochastic properties, are necessary.

With equations (13) and (17), the upper bound observer is designed [Krebs et al. (2016a)],

$$\dot{\overline{\hat{x}}}(t) = (A - LC) \cdot \overline{\hat{x}}(t) + B \cdot \hat{\beta}_c(t) + \overline{L \cdot [\beta_{i,n}]}(t), \tag{18}$$

and the lower bound observer is also designed [Krebs et al. (2016a)],

$$\dot{\underline{\hat{x}}}(t) = (A - LC) \cdot \underline{\hat{x}}(t) + B \cdot \hat{\beta}_c(t) + \underline{L \cdot [\beta_{i,n}]}(t). \tag{19}$$

To solve $\underline{L \cdot [\beta_{i,n}]}$ and $\overline{L \cdot [\beta_{i,n}]}$ in equations (18) and (19) the mathematical approach proposed in [Efimov et al. (2012); Krebs et al. (2016a)] is used, leading to:

$$[\underline{L \cdot [\beta_{i,n}]}, \overline{L \cdot [\beta_{i,n}]}] = [L^+ \cdot \underline{\beta_{i,n}} + L^- \overline{\beta_{i,n}}, L^+ \cdot \overline{\beta_{i,n}} + L^- \cdot \underline{\beta_{i,n}}], \tag{20}$$

where, $L^+ = max\{0, L\}$ and $L^- = L^+ - L$.

Finally, we can state the design conditions for the interval observer:

Problem: Find a gain value of L (for each case) such that:

(1) the linear observers in equations (18) and (19) are positive, i.e. $A - LC$ is Metzler [Krebs et al. (2016b)];
(2) the linear observers in equations (18) and (19) are asymptotically stable, i.e. $A - LC$ is Hurwitz stable [Krebs et al. (2016b)];

The chosen observers eigenvalues are, for all cases, $\lambda_1 = -2.64339$ and $\lambda_2 = -17.6887$. The computed L values, for each case, are thus

$$L_{FF} = \begin{pmatrix} 7 \\ -170 \end{pmatrix}, \tag{21}$$

$$L_{F1} = \begin{pmatrix} 15.1750 \\ -64.3338 \end{pmatrix}, \tag{22}$$

$$L_{F2} = \begin{pmatrix} 9.4270 \\ -108.8978 \end{pmatrix}, \tag{23}$$

$$L_{F3} = \begin{pmatrix} 14.1760 \\ -52.2073 \end{pmatrix}, \tag{24}$$

where L_{FF}, L_{F1}, L_{F2}, and L_{F3} are the L gains of the fault-free, fault 1, fault 2, and fault 3 interval observers, see Table 2.

Remark: in this work, the eigenvalues are selected by experience and trial-and-error but not finely tuned.

3.2 Residual generation and postprocess

In this work the most important role of the interval observers is to generate a residual signal which includes the random noise.

We propose the following residual signals r_i(t)

$$r_i(t) = \beta_{i,n}(t) - \overline{\hat{x}_i}(t), \quad i = 0, 1, 2, 3, \tag{25}$$

where r_i(t) are the residual signals generated using the estimated upper bound pitch position values $\overline{\hat{x}_i}$ of the FF ($i = 0$), F1 ($i = 1$) F2 ($i = 2$) and F3 ($i = 3$) interval observers.

A residual postprocess block as described in Figure 3, is finally applied to determine if any faults have ocurred.

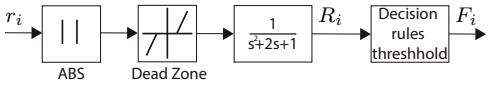

Fig. 3. Postprocess of the residual signal. r_i (t), to obtain a new signal. R_i (t), where decision rules are applied. Note that the Simulink dead zone block is used (start of dead zone value equal to zero and end of dead zone value equal to 0.0007).

The decision rules (thresholds) to pinpoint the type of fault are:

- If the FF interval observer leads to a R_0(t) less than $4.26 \cdot 10^{-5}$, means that the pitch actuator is healthy, otherwise a fault is detected.
- If the F1 interval observer leads to a R_1 (t) less than $2 \cdot 10^{-5}$, then a high air content in oil fault exists.
- If the F2 interval observer leads to a R_2 (t) less than $3.3 \cdot 10^{-5}$, means that a pump wear fault exists.
- If the F3 interval observer leads to a R_3 (t) less than $1.99 \cdot 10^{-5}$, then a hidraulic leakage fault exists.

Finally, Figure 4 shows the closed-loop system.

4. DIAGNOSIS RESULTS

To demonstrate the performance of the proposed diagnosis algorithm, the four different operations modes (as given in Table 2) are regarded. For each of the four system models, FF, F1, F2, and F3, interval observers as described in Section 3 are implemented and initialized with the initial state. The output uncertainty n(t) is a white noise signal that lies between [-0.004. 0.004].

In the simulations, the faults are introduced only in the third pitch actuator β_3 (thus β_1 and β_2 are fault-free) in the following way. From $t = 0$s to $t = 100$s, it is fault free (FF). From $t = 100$s to $t = 101$s, a fault due to high air content in oil (F1) is linearly introduced. From $t = 101$s to $t = 201$s, F1 is fully active. From $t = 201$s to $t = 202$s, F1 is linearly eliminated. From $t = 202$s to $t = 302$s, it is fault free. From $t = 302$s to $t = 322$s, a fault due to pump wear (F2) is linearly introduced. From $t = 322$s to $t = 422$s, F2

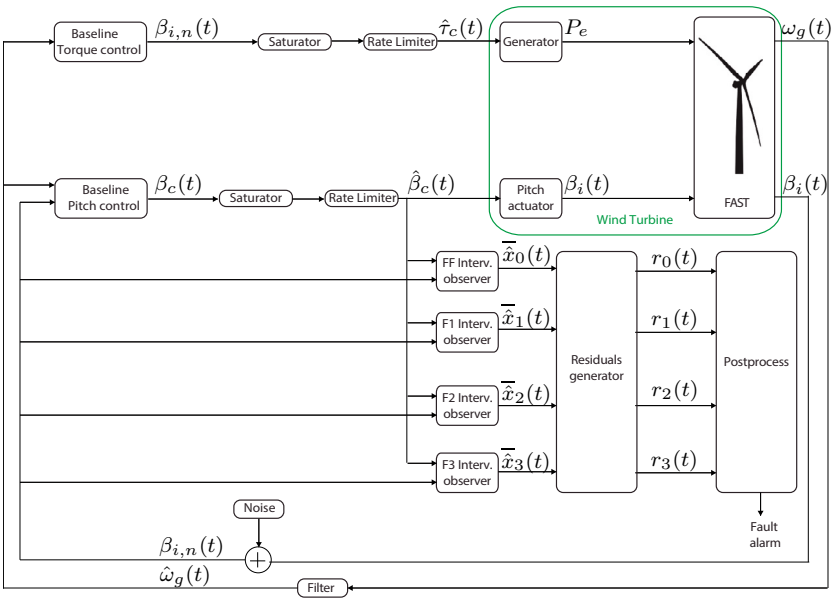

Fig. 4. Block diagram of the closed loop system with the proposed FDI strategy.

is fully active. From $t = 422$s to $t = 442$s, F2 is linearly eliminated. From $t = 442$s to $t = 542$s, it is fault free. From $t = 542$s to $t = 562$s, a fault due to hydraulic leakage (F3) is linearly introduced. From $t = 562$s to $t = 662$s, F3 is fully active. From $t = 662$s to $t = 682$s, F3 is linearly eliminated. From $t = 682$s to $t = 700$s, it is fault free. Figure 5 shows how the studied faults are introduced in the simulations.

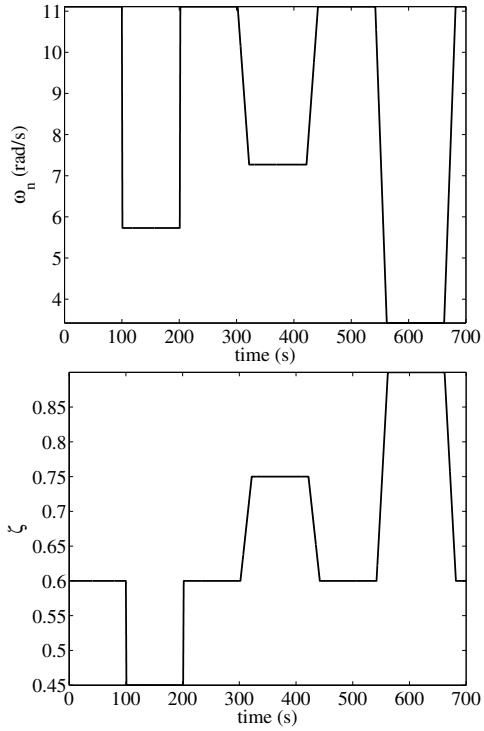

Fig. 5. Variation of ω_n (top) and ζ (bottom) in faulty case.

Figures 6, 7, 8 and 9 show the residual signals generated by the interval observers and their respective computed signals. It can be seen from Figure 6 that when the system is fault-free the residual signal R_0 is close to zero. On the other hand, when a fault appears, it is significantly affected.

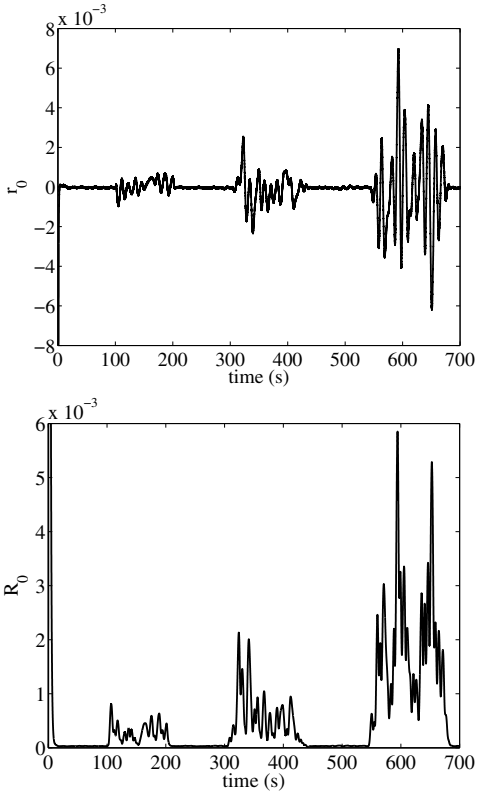

Fig. 6. FF interval observer residual signal (top) and its postprocessed signal (bottom).

As can be seen in Figure 7 the fault F1 can be isolated whith its respective interval observer postprocessed residual signal R_1 when its less than the stablished threshold.

Figure 8 shows the postpropocessed residual signal R_2 that allows to isolate the F2 between 302 to 542s.

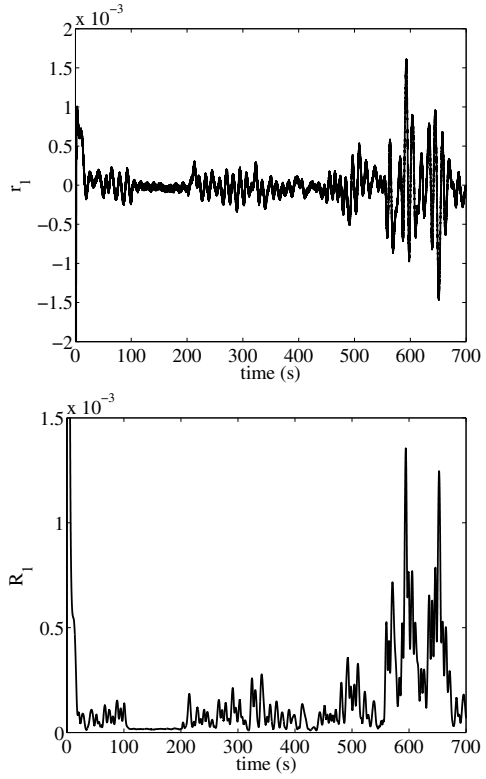

Fig. 7. F1 interval observer residual signal (top) and its postprocessed signal (bottom).

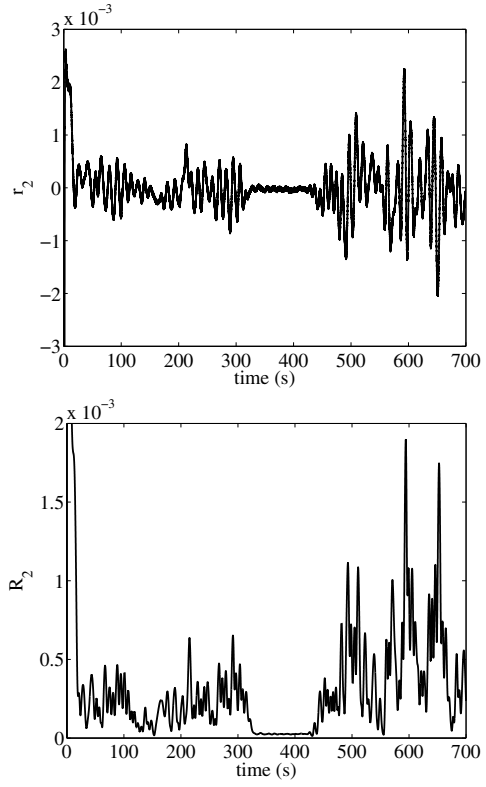

Fig. 8. F2 interval observer residual signal (top) and its postprocessed signal (bottom).

Finally, when R_3 is less than $1.99 \cdot 10^{-5}$ the F3 is isolated (see Figure 9).

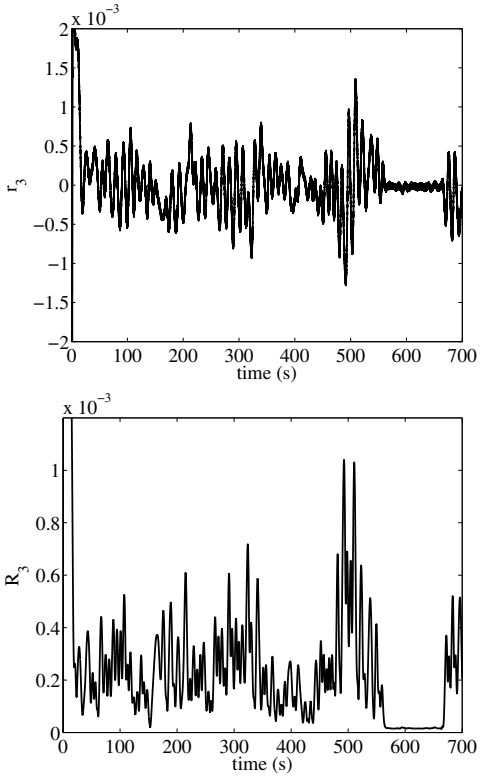

Fig. 9. F3 interval observer residual signal (top) and its postprocessed signal (bottom).

In general, the amount of time needed for fault detection and isolation after the occurrence of a fault is related to the fault strength as well as the amount of uncertainty in the system models [Wolff et al. (2008)]. Here, it is possible to detect and isolate the studied faults before they are fully active (during the linear introduction).

5. CONCLUSIONS

We have presented the design of interval observers to detect and isolate pitch actuator faults in WTs. Three pitch actuator faults are studied. Any fault in the pitch actuator that implies a change in the dynamics will be detected using this method. Simulations demonstrated the performance of the presented method for the state estimation and FDI in WTs. In general the FF interval observer detects when exist a pitch actuator fault (fault detection) and with the F1, F2 and F3 interval observers the respective faults can be isolated (fault isolation). One problem found is that the pitch actuator input signal is saturated and limited, and this method need a permanent excitement input. For this reason, it is unclear, for the moment, how to introduce more noise to the pitch position sensor, but some future works will design an infinity filter to reduce this noise and use linear matrix inequalities methods taking into account the noise when the value of the gain L is calculated. These questions are left for future research.

REFERENCES

Besançon, G. (2003). High-gain observation with disturbance attenuation and application to robust fault detection. *Automatica*, 39(6), 1095–1102.

Blesa, J., Rotondo, D., Puig, V., and Nejjari, F. (2014). FDI and FTC of wind turbines using the interval observer approach and virtual actuators/sensors. *Control Engineering Practice*, 24, 138–155.

Briat, C. and Khammash, M. (2016). Interval peak-to-peak observers for continuous-and discrete-time systems with persistent inputs and delays. *Automatica*, 74, 206–213.

Chaaban, R., Ginsberg, D., and Fritzen, C.P. (2014). Structural load analysis of floating wind turbines under blade pitch system faults. In *Wind Turbine Control and Monitoring*, 301–334. Springer.

Chen, J. and Patton, R.J. (2012). *Robust model-based fault diagnosis for dynamic systems*, volume 3. Springer Science & Business Media.

Chen, W., Ding, S.X., Haghani, A., Naik, A., Khan, A.Q., and Yin, S. (2011). Observer-based FDI schemes for wind turbine benchmark. *IFAC Proceedings Volumes*, 44(1), 7073–7078.

Dong, J. and Verhaegen, M. (2011). Data driven fault detection and isolation of a wind turbine benchmark. *IFAC Proceedings Volumes*, 44(1), 7086–7091.

Edwards, C., Spurgeon, S.K., and Patton, R.J. (2000). Sliding mode observers for fault detection and isolation. *Automatica*, 36(4), 541–553.

Efimov, D., Fridman, L., Raissi, T., Zolghadri, A., and Seydou, R. (2012). Interval estimation for LPV systems applying high order sliding mode techniques. *Automatica*, 48(9), 2365–2371.

Gouzé, J.L., Rapaport, A., and Hadj-Sadok, M.Z. (2000). Interval observers for uncertain biological systems. *Ecological modelling*, 133(1), 45–56.

Gsanger, S. and Pitteloud, J.D. (2012). World wind energy report 2011. *World Wind Energy Association, Bonn, Germany*.

Jonkman, B.J. (2009). *TurbSim user's guide: Version 1.50*. National Renewable Energy Laboratory (NREL). URL `https://nwtc.nrel.gov/turbsim`.

Jonkman, J., Butterfield, S., Musial, W., and Scott, G. (2009). Definition of a 5-mw reference wind turbine for offshore system development. Technical report, National Renewable Energy Laboratory (NREL).

Jonkman, J.M., Buhl Jr., M.L., et al. (2005). Fast user's guide. Technical report, National Renewable Energy Laboratory (NREL).

Jonkman, J.M. (2007). Dynamics modeling and loads analysis of an offshore floating wind turbine. *National Renewable Energy Laboratory*, 68, 233.

Jonkman, J.M. (2010). *Definition of the floating system for phase IV of OC3*. National Renewable Energy Laboratory.

Kapila, V. and Grigoriadis, K. (2002). *Actuator saturation control*. CRC Press.

Kiasi, F., Prakash, J., Shah, S., and Lee, J.M. (2011). Fault detection and isolation of a benchmark wind turbine using the likelihood ratio test. *IFAC Proceedings Volumes*, 44(1), 7079–7085.

Krebs, S., Pfeifer, M., Fugel, S., Weigold, J., and Hohmann, S. (2016a). Interval observer for LPV systems based on time-variant transformations. In *Decision and Control (CDC), 2016 IEEE 55th Conference on*, 4090–4096. IEEE.

Krebs, S., Schnurr, C., Pfeifer, M., Weigold, J., and Hohmann, S. (2016b). Reduced-order hybrid interval observer for verified state estimation of an induction machine. *Control Engineering Practice*, 57, 157–168.

Larsen, T.J. and Hanson, T.D. (2007). A method to avoid negative damped low frequent tower vibrations for a floating, pitch controlled wind turbine. *Journal of Physics: Conference Series*, 75, 1–11.

Leithead, W. and Dominguez, S. (2005). Controller design for the cancellation of the tower fore-aft mode in a wind turbine. In *Conference on Decision and Control and European Control Conference*, volume 44, 1276–1281. IEEE.

Liberatore, S., Speyer, J.L., and Hsu, A.C. (2006). Application of a fault detection filter to structural health monitoring. *Automatica*, 42(7), 1199–1209.

Odgaard, P.F. and Johnson, K.E. (2013). Wind turbine fault detection and fault tolerant control-an enhanced benchmark challenge. In *American Control Conference (ACC), 2013*, 4447–4452. IEEE.

Odgaard, P.F., Sánchez Sardi, H.E., Escobet Canal, T., and Puig Cayuela, V. (2015). Fault diagnosis and fault tolerant control with application on a wind turbine low speed shaft encoder. In *SAFEPROCESS 9th IFAC Symposium on Fault Detection, Supervision and Safety for Technical Processes*, 1357–1362. IFAC.

Odgaard, P.F., Stoustrup, J., and Kinnaert, M. (2013). Fault-tolerant control of wind turbines: A benchmark model. *IEEE Transactions on Control Systems Technology*, 21(4), 1168–1182.

Pisu, P. and Ayalew, B. (2011). Robust fault diagnosis for a horizontal axis wind turbine. *IFAC Proceedings Volumes*, 44(1), 7055–7060.

Puig, V., Quevedo, J., Escobet, T., Morcego, B., and Ocampo, C. (2004). Control tolerante a fallos (parte i): Fundamentos y diagnóstico de fallos. *Revista Iberoamericana de Automática e Informática Industrial*, 1(1), 15–31.

Puig, V., Quevedo, J., and Tornil, S. (2000). Robust fault detection: active versus passive approaches. In *IFAC Symposium on Fault Detection Supervision and Safety for Technical Process*, 155–161.

Rapaport, A. and Gouzé, J. (2003). Parallelotopic and practical observers for non-linear uncertain systems. *International journal of control*, 76(3), 237–251.

Sanchez, H., Escobet, T., Puig, V., and Odgaard, P.F. (2015). Fault diagnosis of an advanced wind turbine benchmark using interval-based arrs and observers. *IEEE Transactions on Industrial Electronics*, 62(6), 3783–3793.

Svärd, C. and Nyberg, M. (2011). Automated design of an FDI-system for the wind turbine benchmark. *IFAC Proceedings Volumes*, 44(1), 8307–8315.

Tavner, P. (2012). Offshore wind turbines: Reliability. *Availability and Maintenance, The Institution of Engineering and Technology, London, UK*.

Vidal, Y., Acho, L., and Pozo, F. (2012). Robust fault detection in hysteretic base-isolation systems. *Mechanical Systems and Signal Processing*, 29, 447–456.

Wolff, F., Krutina, P., and Krebs, V. (2008). Robust consistency-based diagnosis of nonlinear systems by set observation. *IFAC Proceedings Volumes*, 41(2), 10124–10129.